

CompNet: Complementary Segmentation Network for Brain MRI Extraction

Raunak Dey, Yi Hong

University of Georgia

Abstract. Brain extraction is a fundamental step for most brain imaging studies. In this paper, we investigate the problem of skull stripping and propose complementary segmentation networks (CompNets) to accurately extract the brain from T1-weighted MRI scans, for both normal and pathological brain images. The proposed networks are designed in the framework of encoder-decoder networks and have two pathways to learn features from both brain tissues and their complementary part located outside of the brain. The complementary pathway extracts the features in the non-brain region and leads to a robust solution to brain extraction from MRIs with pathologies, which do not exist in our training data set. We demonstrate the effectiveness of our networks by evaluating them on the OASIS data set, resulting in the state of the art performance under the two-fold cross-validation setting. Moreover, the robustness of our networks is verified by testing on images with introduced pathologies and by showing its invariance to unseen brain pathologies. In addition, our complementary network design is general and can be extended to address other image segmentation problems with better generalization.

1 Introduction

Image segmentation, which is used to locate and extract objects of interest from the image, is one of the fundamental problems in medical research. Take the brain extraction problem as an example. To study the brain, magnetic resonance imaging (MRI) is the most popular modality choice. However, before the quantitative analysis of brain MRIs, e.g., measuring normal brain development and degeneration, uncovering brain disorders such as Alzheimer’s disease, or diagnosing brain tumors or lesions, skull stripping is typically a preliminary but important step and many approaches have been proposed to tackle this problem.

In literature, the approaches developed for brain MRI extraction can be divided into two categories: traditional methods (manual, intensity or shape model based, hybrid, and PCA-based methods [2,10]) and deep learning methods [6,9]. Deep neural networks have demonstrated the improved quality of the predicted brain mask, compared to traditional methods. However, these deep networks focus on learning image features mainly for brain tissues from a training data set, which is typically a collection of normal (or apparently normal) brain MRIs, because these images are more commonly available than brain scans with pathologies. Thus, their model performance is sensitive to unseen pathological tissues.

In this paper, we propose a novel deep neural network architecture for skull stripping from brain MRIs, which can improve the performance on brain extraction from (apparently) normal images and is insensitive to brain pathology. In this new design, a network learns features for both brain and non-brain tissues, that is, we consider the complementary information of an object, the one outside of the region of interest in the image. For instance, the region outside of the brain, the skull, is highly similar and consistent among the normal and pathological brain images. This complementary knowledge about the brain can help increase the robustness of a brain extraction method and make it able to handle images with unseen structures in the brain.

We explore several complementary segmentation networks (CompNets). In general, the networks have two pathways in common: one to learn what are the brain tissues and to generate a brain mask; the other to learn what are outside of the brain and to help generate a better brain mask. Depending on if there is an extra step to generate the ground truth for the complementary part like the skull and if dense blocks (a series of convolution layers fully connected to each other [3]) and multiple intermediate outputs are used in the network, we have three variants: probability, plain, and optimal CompNets. Among them, the one shown in Fig. 1, without the need of the complementary ground truth but with dense blocks and intermediate outputs, is the optimal one. It has an end-to-end design, less number of parameters to estimate, and the best performance on both normal and pathological images from the OASIS data set. In addition, this network is generic and can be applied in image segmentation if the complementary part of an object contributes to the understanding of the object in the image.

2 CompNets: Complementary Segmentation Networks

An encoder-decoder network, like U-Net [8], is often used in image segmentation. Current segmentation networks mainly focus on objects of interest, which may lead to the difficulty in its generalization to unseen image data. In this section, we introduce our novel complementary segmentation networks (short for CompNet), which increase the segmentation robustness by incorporating the learning process of the object of interest with the learning of its complementary part in the image.

The architecture of our optimal CompNet is depicted in Fig. 1. This network has three components, a segmentation branch for the region of interest (ROI, e.g., the brain), another segmentation branch for the ROI's complementary part (e.g., anything outside of the brain), and a sub-encoder-decoder network to reconstruct the input image based on the outputs of those two segmentation branches. This reconstruction sub-network is designed to guide the learning process of the complementary branch due to its lack of ground-truth, similar to the unsupervised W-Net [12]. That is, in order to guarantee the performance of the reconstruction network, which is built upon the ROI and its complementary branches, the complementary branch should learn useful features for structures outside of the brain. In this way, its output can be integrated with the output of the

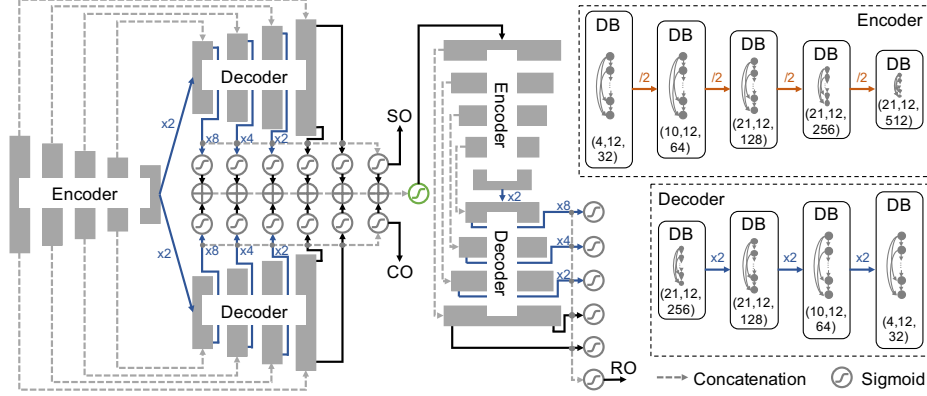


Fig. 1. Architecture of our complementary segmentation network (CompNet) with dense blocks and multiple intermediate outputs. The dense blocks (DB), corresponding to the gray bars, are used in each encoder and decoder. The triple (x, y, z) in each dense block indicates that it has x convolution layers with a kernel size 3×3 ; each layer has y convolution filters, except for the last one that has z filters. SO: segmentation output for the brain mask; CO: complementary segmentation output for the non-brain mask; RO: reconstruction output for the input image. These three outputs produced by the Sigmoid function are the final ones for prediction; while all other Sigmoids produce intermediate outputs, except for the green one that generates an input for the image reconstruction sub-network. Best viewed in color.

ROI segmentation branch, which is guided by the true brain mark, in order to reconstruct a coarse version of the input image.

This optimal CompNet includes dense blocks and multiple intermediate outputs, which help reduce the number of parameters to estimate and make the network easier to optimize. For readability and a better understanding, before discussing this optimal one, we start with a plain CompNet.

Plain CompNet. The plain network is a simplified version of the network shown in Fig. 1, but without dense blocks or multiple intermediate outputs. Similar to U-Net, the encoder and decoder blocks (the gray bars in Fig. 1) of the segmentation and reconstruction sub-networks have two convolutional layers in each, with a kernel of size 3×3 . The number of convolution filters in the encoder starts from 32, followed by 64, 128, 256, and 512, while the number in the decoder starting from 256, followed by 128, 64, and 32. Each convolution layer is followed by batch normalization [4] and dropout [11]. After each gray bar in the encoder, the feature maps are downsampled by 2 using max pooling; while for the decoder the feature maps are upsampled by 2 using deconvolution layers. Each segmentation branch of this plain network has only one final output from the last layer of the decoder, after applying the Sigmoid function. The two outputs of the segmentation branches are combined through addition and passed as input to the reconstruction sub-network. In this sub-network, the output from the last layer of the decoder is the reconstructed image. In addition, as U-Net

we have the concatenation of feature maps from an encoder to its corresponding decoder at the same resolution level, as indicated by the gray arrows in Fig. 1.

To build the objective function, we use the dice coefficient ($Dice(A, B) = 2|A \cap B|/(|A| + |B|)$ [1]) to measure the goodness of the results from two segmentation branches and the mean squared error (MSE) to measure the goodness of the reconstruction result. In particular, the learning goal of this plain network is to maximize the dice coefficient between the predicted mask for the ROI (\hat{Y}_S) and its ground truth (Y_S), minimize the dice coefficient between the predicted mask for the non-ROI (\hat{Y}_C) and the ground truth of the ROI, and minimize the MSE between the reconstructed image (\hat{X}_R) and the original input image (X). The loss function for one sample to minimize is formulated as:

$$Loss(Y_S, \hat{Y}_S, \hat{Y}_C, X, \hat{X}_R) = -Dice(Y_S, \hat{Y}_S) + Dice(Y_S, \hat{Y}_C) + MSE(X, \hat{X}_R). \quad (1)$$

Here, X and Y_S are given, while \hat{Y}_S , \hat{Y}_C , and \hat{X}_R are outputs from the network.

Optimal CompNet. The plain CompNet has nearly 18 million parameters. Introducing dense connections among convolution layers can greatly reduce the number of parameters of a network and mitigate the vanishing gradient problem in a deep neural network. Therefore, we replace each gray block in the plain CompNet with a dense block, as shown in Fig. 1. Each dense block has different numbers of convolution layers and filters. Specifically, the dense blocks in each encoder have 4, 10, 21, 21, and 21 convolution layers, respectively, and the ones in each decoder have 21, 21, 10, and 4 layers, respectively. All these convolution layers use the same kernel size 3×3 and the number of convolution filters is 12 in each layer, except for the last one, changing from 32, to 64, to 128, to 256, and to 512 in the five dense blocks of the encoder while changing from 256, to 128, to 64, and to 32 in the four dense blocks of the decoder. This design aims to increase the amount of information that is transferred from one dense block to its next one by using more feature maps. In addition, dropout is applied at the transition between dense blocks. Through adopting these dense blocks, our optimal CompNet becomes much deeper while having less parameters (15.3 million) to optimize, compared to the plain one.

Another change we make to the plain CompNet is introducing multiple intermediate outputs, which is another strategy to mitigate the vanishing gradient problem in a deep neural network, by shorting the distance from the input to the output. As shown in Fig. 1, each decoder in the segmentation and reconstruction sub-networks has six outputs, one after each Sigmoid function. The first five outputs are generated from the original or up-sampled feature maps of the first convolution layer in each dense block of the decoder, or from the feature maps of the last convolution layer in the last dense block. These five outputs are treated as the intermediate outputs during the training. The sixth output is generated from the concatenation of all feature maps used for the intermediate outputs and is treated as the final output of that branch for prediction. Furthermore, each corresponding intermediate or final output from the two segmentation branches is combined by an addition operation and all of them are then concatenated and

passed through a Sigmoid function to generate the input for the reconstruction sub-network. Note that, this sigmoid function has no intermediate output. In addition, each Sigmoid layer reduces the channel number of feature maps to be 1, summarizes and normalizes the response value in features maps within $[0, 1]$.

Probability CompNet. The reconstruction sub-network is to guide the learning process of the complementary pathway. One might replace it by providing the ground truth of the complementary part for training, e.g., generating the skull masks. This is our first attempt and it could be non-trivial for images with very noisy background. After having true masks for both brain and non-brain segmentation branches, we can build a network containing only the segmentation part as in Fig. 1, without the reconstruction part. To leverage the complementary information, we can build connections between the two segmentation branches for the convolution layers at the same resolution level. In particular, the feature maps of a block from one segmentation branch are converted to a probability map, which is inverted and then multiplied to the feature maps at the same resolution level of the other branch. We do the same operations on the other branch. Essentially, one branch informs the other one to focus on learning features of its complementary part. This complementary segmentation network with connections through probability maps is named as probability CompNet. It can also handle brain extraction from pathological images; however, both brain and skull masks are required for training and the image background noise will influence the result. Although an intensity threshold can be set to denoise the image background, this hyper-parameter may vary among images collected from different brain MRI scanners.

3 Experiments

Data Sets. We evaluate CompNets on the OASIS data set [7], which consists of a collection of T1-weighted brain MRI scans of 416 subjects aged 18 to 96 and 100 of them over the age of 60 clinically diagnosed mild to moderate Alzheimer’s disease. We use a subset with 406 subjects which have both brain images and brain masks available, with image dimension of $256 \times 256 \times 256$. The subjects in this subset are randomly shuffled and equally divided into two chunks for training and testing with two-fold cross-validation, similar to [6] for performance comparison on (apparently) normal brain images.

To further evaluate the robustness of our networks, in one chunk of the OASIS subset we introduce brain pathologies, such as synthetic 3D brain tumors and lesions with different intensity distributions, into the images at different locations and with different sizes, as well as damaged skull and non-brain tissue membrane, as shown in the first image column of Fig. 2. We train networks on the other chunk of unchanged images and test them on this chunk of noisy images.

Experimental Settings. The networks are implemented in Keras with TensorFlow as backend. To overcome the overfitting issue, apart from a dropout

	(Apparently) Normal Images			Pathological Images		
	Dice	Sensitivity	Specificity	Dice	Sensitivity	Specificity
Kleesiek et al. [6]*	95.77±0.01	94.25±0.03	99.36±0.003	—	—	—
Plain U-Net	92.30±6.20	95.60±1.48	96.20±0.09	79.90±8.10	93.80±5.10	95.20±2.15
Dense U-Net	96.40±4.10	97.50±0.70	96.90±0.01	85.43±5.80	96.13±3.20	97.10±1.27
Prob. CompNet	95.10±0.19	96.73±0.90	96.03±0.02	92.10±5.23	96.32±1.90	98.86±0.50
Plain CompNet	96.70±0.22	97.93±0.62	98.57±0.06	95.21±3.75	96.32±1.03	99.21±0.10
Opti. CompNet	98.27±0.30	98.26±0.58	99.80±0.05	97.62±2.21	97.84±0.80	99.76±0.12

Table 1. Quantitative comparison (mean and standard deviation in percentage) among different networks on (apparently) normal and pathological images. *This paper is not directly comparable to our networks, because it was evaluated on mixed data samples, including 77 images (57%) from OASIS data set. (Prob.: Probability; Opti.: Optimal).

rate of 0.3 as discussed in Section 2, we also use L_2 regularizer to penalize network weights with large magnitudes and its control hyperparameter λ is set to $2e-4$. For training, we use the Adam optimizer [5] with a learning rate $1e-3$. All networks run up to 10 epochs.

Experimental Results. We compare our CompNets with a 3D deep network proposed in [6], a plain U-Net that the plain CompNet is built on (see Section 2), and a dense U-Net that the optimal CompNet is built on. These networks are tested on (apparently) normal images (with 2-fold cross-validation) and on pathological images (with being trained on the other fold with normal images). Given a 3D brain MRI scan of a subject, our networks accept 2D slices and predict their brain masks slice by slice, which are then stacked back to a 3D mask without any post-processing. We use Dice score, sensitivity, and specificity to quantify the segmentation performance of the networks, as reported in Table 1. Our optimal CompNet consistently performs the best among all networks for either normal (averaged Dice of 98.27%) or pathological (averaged Dice 97.62%) images, although its performance on images with pathologies is slightly downgraded by less than 0.7% on average and less than 2.6% in the worst case.

The visual comparison of the predicted brain masks has been demonstrated in Fig. 2. For (apparently) normal brain scans, all networks produce visually acceptable brain masks. However, the basic and dense U-Nets have difficulty in handling images with pathologies, especially pathological tissues that are on or near the boundary of the brain. Part of the pathological tissues in the brain are considered as non-brain tissues. The plain U-Net even oversegments the skull as part of the brain if the skull intensity changes, as shown in the case 3 of Fig. 2. In contrast, our CompNets can correctly recognize the brain and the optimal CompNet presents the best results on all four cases.

Furthermore, in Fig. 3 we show the three outputs from the optimal CompNet: the brain and its complementary masks and the reconstructed image. According to the combination of the brain mask and its complementary one, we can identify different parts in the brain image. This confirms that the brain branch works as expected; more importantly, the complementary branch has learned features for

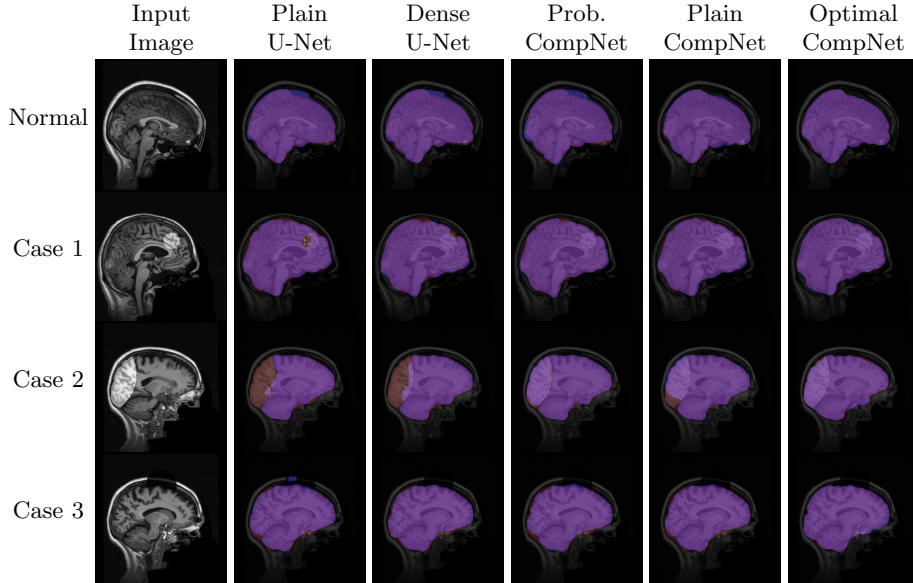


Fig. 2. Visual comparison among five networks, plain and dense U-Nets, probability, plain, and optimal CompNets, on four image samples, a normal one, one with pathology inside of the brain (case 1), one with pathology on the boundary of the brain (case 2), and one with damaged skull (case 3). The true (red) and predicted (blue) masks are superimposed over the original images. The purple color indicates a perfect overlap between the ground truth and the prediction. Best viewed in color.

separating the non-brain region from the brain tissues. This enables the network to handle unseen brain tissues and be insensitive to pathologies in images.

4 Discussion and Conclusions

In this paper, we proposed a complementary network architecture to segment brain out from a brain MRI scan. We observed that the complimentary segmentation branch of the optimal CompNet learns a mask outside of the brain and can help recognize different structures in the non-brain region. This enables our network to be insensitive to brain images with pathologies and correctly segment the brain, including the pathological tissues inside or on the boundary of the brain. Our experiments use synthetic pathological images due to the lack of publicly available brain images with both pathology and skull; however, we will make our source code and trained networks publicly available for others to use.

Furthermore, our current networks accept 2D slices from a 3D brain image, but they can be extended to 3D networks for directly handling 3D images. Implementing 3D CompNets will be one of our future work plans. In addition, our complementary network design is not specific to the brain extraction problem but can be generalized to other image segmentation problems if the complemen-

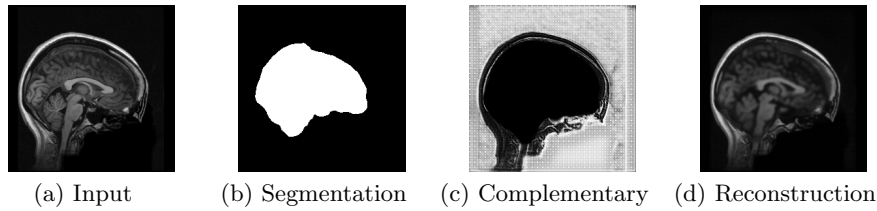


Fig. 3. Three outputs (b-d) from our optimal CompNet for the input image (a). The large white region in (c) is unsmooth because of the noisy image background in (a).

tary part helps learn and understand the objects of interest. The generalization of our networks to other segmentation applications will also be our future work.

References

1. Dice, L.R.: Measures of the amount of ecologic association between species. *Ecology* 26(3), 297–302 (1945)
2. Han, X., Kwitt, R., Aylward, S., Menze, B., Asturias, A., Vespa, P., Van Horn, J., Niethammer, M.: Brain extraction from normal and pathological images: A joint PCA/image-reconstruction approach. *arXiv preprint arXiv:1711.05702* (2017)
3. Huang, G., Liu, Z., Weinberger, K.Q., van der Maaten, L.: Densely connected convolutional networks. In: *Proceedings of the IEEE conference on computer vision and pattern recognition*. vol. 1, p. 3 (2017)
4. Ioffe, S., Szegedy, C.: Batch normalization: Accelerating deep network training by reducing internal covariate shift. In: *ICML*. pp. 448–456 (2015)
5. Kingma, D.P., Ba, J.: Adam: A method for stochastic optimization. *arXiv preprint arXiv:1412.6980* (2014)
6. Kleesiek, J., Urban, G., Hubert, A., Schwarz, D., Maier-Hein, K., Bendszus, M., Biller, A.: Deep MRI brain extraction: a 3d convolutional neural network for skull stripping. *NeuroImage* 129, 460–469 (2016)
7. Marcus, D.S., Wang, T.H., Parker, J., Csernansky, J.G., Morris, J.C., Buckner, R.L.: Open access series of imaging studies (OASIS): cross-sectional MRI data in young, middle aged, nondemented, and demented older adults. *Journal of cognitive neuroscience* 19(9), 1498–1507 (2007)
8. Ronneberger, O., Fischer, P., Brox, T.: U-net: Convolutional networks for biomedical image segmentation. In: *International Conference on Medical image computing and computer-assisted intervention*. pp. 234–241. Springer (2015)
9. Salehi, S.S.M., Erdogmus, D., Gholipour, A.: Auto-context convolutional neural network for geometry-independent brain extraction in magnetic resonance imaging. *arXiv preprint arXiv:1703.02083* (2017)
10. Souza, R., Lucena, O., Garrafa, J., Gobbi, D., Saluzzi, M., Appenzeller, S., et al.: An open, multi-vendor, multi-field-strength brain MR dataset and analysis of publicly available skull stripping methods agreement. *NeuroImage* (2017)
11. Srivastava, N., Hinton, G., Krizhevsky, A., Sutskever, I., Salakhutdinov, R.: Dropout: A simple way to prevent neural networks from overfitting. *The Journal of Machine Learning Research* 15(1), 1929–1958 (2014)
12. Xia, X., Kulis, B.: W-net: A deep model for fully unsupervised image segmentation. *arXiv preprint arXiv:1711.08506* (2017)